Supplementary Information

Asymmetric Fiber Supercapacitors Based on a FeC_2O_4/FeOOH-CNT Hybrid Material

Paa Kwasi Adusei [a], Kevin Johnson [b], Sathya Kanakaraj [a], Guangqi Zhang [a], Yanbo Fang [a], Yu-Yun Hsieh [a], Mahnoosh Khosravifar [a], Seyram Gbordzoe [a], Matthew Nichols [b], Vesselin Shanov [a, b] *

[a] Department of Mechanical and Materials Engineering, University of Cincinnati, Cincinnati, OH, 45221-0072, USA

[b] Department of Chemical and Environmental Engineering, University of Cincinnati, OH, 45221-0012, USA
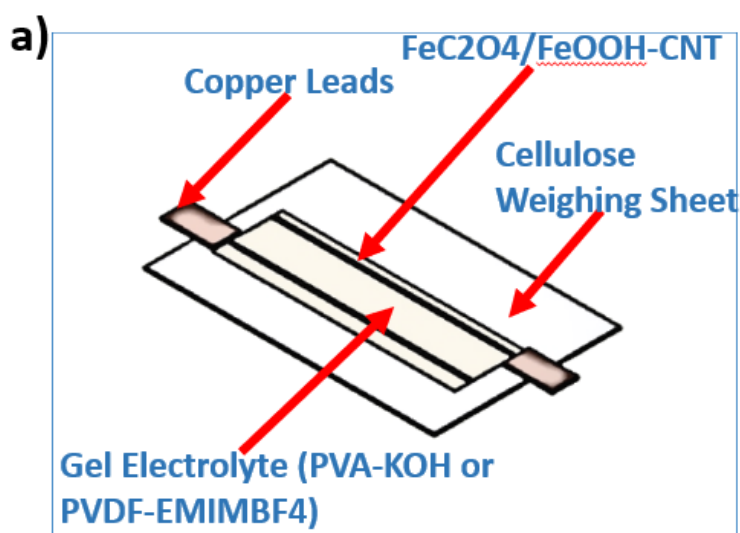
[*] Corresponding author: Vesselin.shanov@uc.edu

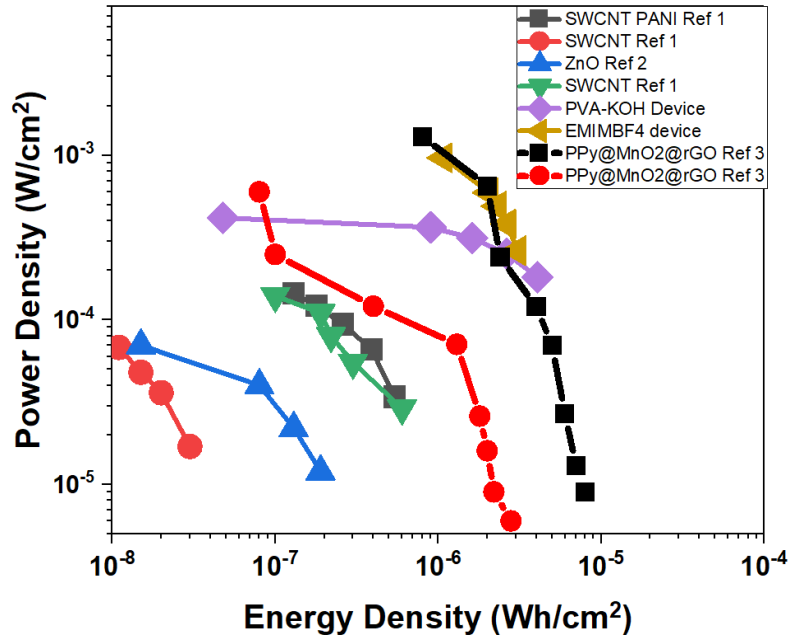**Figure S1**. Schematic of the supercapacitor.

Figure S2. Ragone plot comparing data generated by our device with data from other devices from the literature [1–3]

Effect of KOH Concentration

In KOH electrolyte, there are several chemical reactions during the device charge and discharge, which are characterized by the oxidation and reduction peaks observed in the CV curves at lower scan rates (Figure S2a). The chemical reactions for charging and discharging are presented below for both FeC_2O_4 and $FeOOH$ [4,5]. It was found that during the charging process, FeC_2O_4 was entirely converted into $Fe(OH)_2$ which was the source of $FeOOH$. On the other hand, $FeOOH$ during discharge generated $Fe(OH)_2$ as presented below.

For charging:

- $FeC_2O_4 + 6OH^- \rightarrow Fe(OH)_2 + 2CO_3^{2-} + 2H_2O + 2e^-$

- $Fe(OH)_2 + OH^- \rightarrow FeOOH + H_2O + e^-$

For discharging

- $FeOOH + H_2O + e^- \rightarrow Fe(OH)_2 + OH^-$

We speculate that the poor cyclability revealed by the KOH devices is due to the chemical reactions that are taking place during the device performance. It has been detailed in the literature that pseudocapacitive materials have poor cyclic stability compared to electric double layer capacitor (EDLC) devices due to the chemical reactions taking place and their physical effects on the electrode [6]. To prove this, we compared our device tested with 1.23M KOH electrolyte with devices we made using a lower and higher electrolyte concentration of 0.61M KOH and 2.5M KOH, respectively. The cycling data from these devices are presented in Figure S2b. This comparison showed that the greater the concentration of the KOH, the worst the cyclability was. The 2.5M KOH device had the lowest cyclability retention rate of 74.93% when tested over 4000 cycles. However, the 0.61M KOH device maintained ~100% capacitance retention at the same cycling conditions. It needs to be point out that the 0.61M KOH device revealed modest energy and power density of $0.101\,\mu Wh/cm^2$ at $167mW/cm^2$, compared to $2.45\,\mu Wh/cm^2$ at $462mW/cm^2$ for the 1.23M KOH device, and $3.386\,\mu Wh/cm^2$ at $475.84mW/cm^2$ for the 2.5M KOH device. These values have been obtained from the charge-discharge curves at current density of $0.5mA/cm^2$. From this data is reasonable to conclude that there is a tradeoff between the device energy parameters and the capacitance retention. The involved chemical reactions using KOH electrolyte were therefore responsible for the improved electrochemical performance, but also contributed to the poorer cyclic stability.
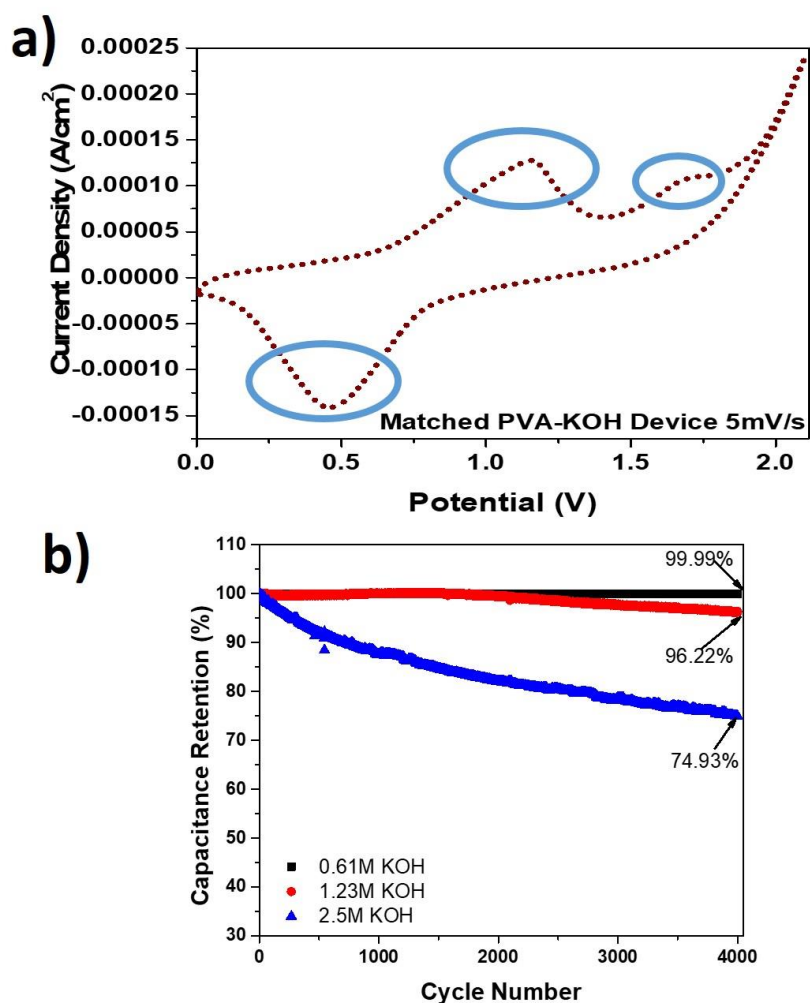
Figure S3. a) CV curve at a scanning rate of 5mV/s highlighting the chemical reactions taking place during charge and discharge; b) Capacitance retention data for KOH devices at different molarities of the electrolyte tested over 4000 cycles.

Table S1. Comparison of Energy Density and Power Density data of our devices with others in literature.

Material	Areal Energy Density (μWh/cm^2)	Areal Power Density (mW/cm^2)	Ref
Graphene Core-Sheath Fiber	0.04-0.17	0.006-0.100	[7]
SWCNT/PANI	~0.13-0.54	~0.0034-0.145	[1]
ZnO-MnO$_2$-CF	~2.8	~0.006	[2]
MnO$_2$-CNT	0.55-1.14	0.210-1.500	[8]

Co3O4@MnO2/Ni	4.34	0.750	[9]
CNF/MW	1.74	0.064	[10]
CNT/RGO	3.80	0.250	[11]
MnO_2-CF	3.26	0.118	[12]
CF-MnO_2 // CF-MoO_3	2.70	0.530	[13]
PEDOT D-TiO_2/Ti	0.44	0.230	[14]
FeC_2O_4/FeOOH-CNT PVA-KOH Device	4.07	0.420	**This work**
FeC_2O_4/FeOOH-CNT PVDF-EMIMBF4 Device	3.06	0.970	**This work**

References

[1]   Q. Meng, K. Wang, W. Guo, J. Fang, Z. Wei, X. She, Thread-like Supercapacitors Based on One-Step Spun Nanocomposite Yarns, Small. 10 (2014) 3187–3193. https://doi.org/10.1002/smll.201303419.

[2]   P. Yang, X. Xiao, Y. Li, Y. Ding, P. Qiang, X. Tan, W. Mai, Z. Lin, W. Wu, T. Li, H. Jin, P. Liu, J. Zhou, C.P. Wong, Z.L. Wang, Hydrogenated ZnO Core-Shell Nanocables for Flexible Supercapacitors and Self-Powered Systems, ACS Nano. 7 (2013) 2617–2626. https://doi.org/10.1021/nn306044d.

[3]   Y. Huang, H. Hu, Y. Huang, M. Zhu, W. Meng, C. Liu, Z. Pei, C. Hao, Z. Wang, C. Zhi, From Industrially Weavable and Knittable Highly Conductive Yarns to Large Wearable Energy Storage Textiles, ACS Nano. 9 (2015) 4766–4775. https://doi.org/10.1021/acsnano.5b00860.

[4]   X. Liu, J. Jiang, L. Ai, Non-precious cobalt oxalate microstructures as highly efficient electrocatalysts for oxygen evolution reaction, J. Mater. Chem. A. 3 (2015) 9707–9713. https://doi.org/10.1039/c5ta01012h.

[5]   K.A. Owusu, L. Qu, J. Li, Z. Wang, K. Zhao, C. Yang, K.M. Hercule, C. Lin, C. Shi, Q. Wei, L. Zhou, L. Mai, Low-Crystalline Iron Oxide Hydroxide Nanoparticle Anode for High-Performance Supercapacitors, Nat. Commun. 8 (2017) 14264. https://doi.org/10.1038/ncomms14264.

[6]   X. Zhao, B.M. Sánchez, P.J. Dobson, P.S. Grant, The Role of Nanomaterials in Redox-Based Supercapacitors for Next Generation Energy Storage Devices, Nanoscale. 3 (2011) 839–855. https://doi.org/10.1039/c0nr00594k.

[7]   Y. Meng, Y. Zhao, C. Hu, H. Cheng, Y. Hu, Z. Zhang, G. Shi, L. Qu, All-Graphene Core-Sheath Microfibers for All-Solid-State, Stretchable Fibriform Supercapacitors and Wearable Electronic Textiles, Adv. Mater. 25 (2013) 2326–2331. https://doi.org/10.1002/adma.201300132.

[8]   P. Xu, B. Wei, Z. Cao, J. Zheng, K. Gong, F. Li, J. Yu, Q. Li, W. Lu, J.H. Byun, B.S. Kim, Y. Yan, T.W. Chou, Stretchable Wire-Shaped Asymmetric Supercapacitors Based on Pristine and MnO2 Coated Carbon Nanotube Fibers, ACS Nano. 9 (2015) 6088–6096. https://doi.org/10.1021/acsnano.5b01244.

[9]   X. Niu, G. Zhu, Z. Yin, Z. Dai, X. Hou, J. Shao, W. Huang, Y. Zhang, X. Dong, Fiber-based all-solid-state asymmetric supercapacitors based on Co3O4@MnO2 core/shell nanowire arrays, J. Mater. Chem. A. 5 (2017) 22939–22944. https://doi.org/10.1039/c7ta07899d.

[10]   G. Zhu, J. Chen, Z. Zhang, Q. Kang, X. Feng, Y. Li, Z. Huang, L. Wang, Y. Ma, NiO nanowall-assisted growth of thick carbon nanofiber layers on metal wires for fiber supercapacitors, Chem. Commun. 52 (2016) 2721–2724. https://doi.org/10.1039/c5cc10113a.

[11]   B. Wang, X. Fang, H. Sun, S. He, J. Ren, Y. Zhang, H. Peng, Fabricating Continuous Supercapacitor Fibers with High Performances by Integrating All Building Materials and Steps into One Process, Adv. Mater. 27 (2015) 7854–7860. https://doi.org/10.1002/adma.201503441.

[12]   N. Yu, H. Yin, W. Zhang, Y. Liu, Z. Tang, M.Q. Zhu, High-performance fiber-shaped all-solid-state asymmetric supercapacitors based on ultrathin MnO2 nanosheet/carbon fiber cathodes for wearable electronics, Adv. Energy Mater. 6 (2016). https://doi.org/10.1002/aenm.201501458.

[13]   J. Noh, C.M. Yoon, Y.K. Kim, J. Jang, High performance asymmetric supercapacitor twisted from carbon fiber/MnO2 and carbon fiber/MoO3, Carbon N. Y. 116 (2017) 470–478. https://doi.org/10.1016/j.carbon.2017.02.033.

[14]   R. Vellacheri, H. Zhao, M. Mühlstädt, A. Al-Haddad, K.D. Jandt, Y. Lei, Rationally Engineered Electrodes for a High-Performance Solid-State Cable-Type Supercapacitor, Adv. Funct. Mater. 27 (2017) 1–7. https://doi.org/10.1002/adfm.201606696.